

Strain and composition distributions in wurtzite InGaN/GaN layers extracted from x-ray reciprocal space mapping

S. Pereira, M. R. Correia, E. Pereira, K. P. O'Donnell, E. Alves, A. D. Sequeira, N. Franco, I. M. Watson, and C. J. Deatcher

Citation: *Appl. Phys. Lett.* **80**, 3913 (2002); doi: 10.1063/1.1481786

View online: <http://dx.doi.org/10.1063/1.1481786>

View Table of Contents: <http://aip.scitation.org/toc/apl/80/21>

Published by the [American Institute of Physics](#)

Articles you may be interested in

[X-ray diffraction reciprocal space mapping study of the thin film phase of pentacene](#)

Applied Physics Letters **90**, 181930 (2007); 10.1063/1.2736193

[Elastic strain relaxation and piezoeffect in GaN-AlN, GaN-AlGaIn and GaN-InGaIn superlattices](#)

Journal of Applied Physics **81**, 6332 (1998); 10.1063/1.364368

[Two-dimensional electron gases induced by spontaneous and piezoelectric polarization charges in N- and Ga-face AlGaIn/GaN heterostructures](#)

Journal of Applied Physics **85**, 3222 (1999); 10.1063/1.369664

[Elastic properties of zinc-blende and wurtzite AlN, GaN, and InN](#)

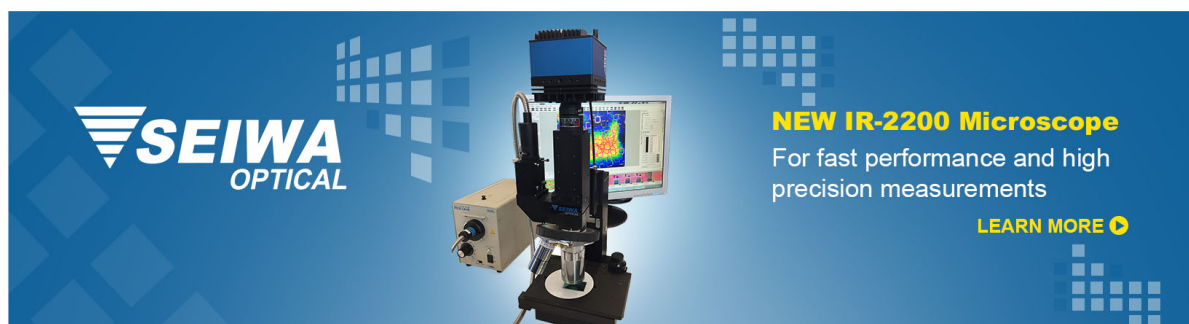
Journal of Applied Physics **82**, 2833 (1998); 10.1063/1.366114

[Calculation of critical layer thickness versus lattice mismatch for \$\text{Ge}_x\text{Si}_{1-x}/\text{Si}\$ strained-layer heterostructures](#)

Applied Physics Letters **47**, 322 (1998); 10.1063/1.96206

[Slip systems and misfit dislocations in InGaIn epilayers](#)

Applied Physics Letters **83**, 5187 (2003); 10.1063/1.1633029



SEIWA
OPTICAL

NEW IR-2200 Microscope
For fast performance and high precision measurements

[LEARN MORE](#)

The advertisement features a blue background with a grid of white squares. In the center, there is a photograph of the SEIWA IR-2200 Microscope, which is a black, boxy device with a camera lens and a small screen. To the left of the microscope is the SEIWA OPTICAL logo, consisting of a stylized 'S' made of horizontal lines followed by the text 'SEIWA OPTICAL'. To the right of the microscope is the text 'NEW IR-2200 Microscope' in bold yellow, followed by 'For fast performance and high precision measurements' in white. At the bottom right, there is a yellow button with the text 'LEARN MORE' and a small yellow circle with a right-pointing arrow.

Strain and composition distributions in wurtzite InGaN/GaN layers extracted from x-ray reciprocal space mapping

S. Pereira^{a)}

Departamento de Física, Universidade de Aveiro, 3810-193 Aveiro, Portugal and Department of Physics, University of Strathclyde, Glasgow G4 0NG, Scotland, United Kingdom

M. R. Correia and E. Pereira

Departamento de Física, Universidade de Aveiro, 3810-193 Aveiro, Portugal

K. P. O'Donnell

Department of Physics, University of Strathclyde, Glasgow G4 0NG, Scotland, United Kingdom

E. Alves, A. D. Sequeira, and N. Franco

Departamento de Física do ITN, E.N. 10, 2686-953 Sacavém, Portugal

I. M. Watson and C. J. Deatcher

Institute of Photonics, University of Strathclyde, Glasgow, United Kingdom

(Received 14 February 2002; accepted for publication 8 April 2002)

Strain and composition distributions within wurtzite InGaN/GaN layers are investigated by high-resolution reciprocal space mapping (RSM). We illustrate the potential of RSM to detect composition and strain gradients independently. This information is extracted from the elongation of broadened reciprocal lattice points (RLP) in asymmetric x-ray reflections. Three $\text{In}_x\text{Ga}_{1-x}\text{N}/\text{GaN}$ (nominal $x=0.25$) samples with layer thickness of 60, 120, and 240 nm, were grown in a commercial metal-organic chemical vapor deposition reactor. The RSMs around the (105) reflection show that the strain profile is nonuniform over depth in InGaN. The directions of “pure” strain relaxation in the reciprocal space, for a given In content (isocomposition lines), are calculated based on elastic theory. Comparison between these directions and measured distributions of the RLP shows that the relaxation process does not follow a specific isocomposition line. The In mole fraction (x) increases as the films relax. At the start of growth all the films have $x\sim 0.2$ and are coherent to GaN. As they relax, x progressively increases towards the nominal value (0.25). Compositional gradients along the growth direction extracted from the RSM analysis are confirmed by complementary Rutherford backscattering measurements. © 2002 American Institute of Physics. [DOI: 10.1063/1.1481786]

Ternary nitride alloys are presently under development for a new generation of light emitters.¹ These semiconductors crystallize preferentially in the hexagonal (wurtzite) structure. Sapphire is the most commonly used substrate, despite the very large lattice mismatch ($\sim 16\%$) between GaN and Al_2O_3 . However, alloy nitride films are not usually grown directly on Al_2O_3 . Usually, an intermediate buffer layer ($\sim 1\ \mu\text{m}$ thick) of GaN is grown, to act as an accommodation layer and to improve crystalline quality. The buffer forms a “virtual substrate” of nearly relaxed GaN. Due to the different lattice constants of GaN, $\text{In}_x\text{Ga}_{1-x}\text{N}$, and $\text{Al}_x\text{Ga}_{1-x}\text{N}$, the alloy films will grow under biaxial compressive or tensile strain.

The most attractive feature of these semiconductors is their efficient luminescence, related to the direct band gap. Additionally, by adjusting the InN content and/or strain in $\text{In}_x\text{Ga}_{1-x}\text{N}$ most of the visible spectral region can, in principle, be covered. However, while efforts in the area of blue-green optoelectronic devices based on InGaN have proved extremely fruitful in recent years,² the growth of layers with high In content ($x>0.2$) remains a challenge. It is therefore important to improve our understanding of the processes hin-

dering In incorporation in the samples, as well as the interplay between strain and composition during growth.

Reciprocal space mapping (RSM) by high-resolution x-ray diffraction is ideally suited to detailed structural characterization of imperfect crystalline layered structures such as nitrides.² However, this technique has rarely been applied to the characterization of InGaN/GaN films.^{3–5} In this letter, we extract key structural parameters of InGaN/GaN layers using asymmetric RSM. Direct evaluation of the local strain state and composition profile in each layer is achieved. We also illustrate the potential of RSM to extract information on the process of In incorporation during InGaN growth.

The samples studied are nominally undoped wurtzite InGaN/GaN layers, grown in an Aixtron 200-series metal-organic chemical vapor deposition reactor on c -plane Al_2O_3 substrates. For InGaN growth at $760\ ^\circ\text{C}$, all gas flows into the reactor were switched from hydrogen to nitrogen. The fluxes of trimethylgallium and trimethylindium were 22.1 and $14.3\ \mu\text{mol/min}$, respectively, and the total V/III ratio was ~ 6100 . The three layers were prepared in consecutive runs, with successive growth periods of 25, 50, and 100 minutes. High-resolution x-ray diffraction was performed in a double crystal diffractometer equipped with a position sensitive detector placed on the 2θ arm. A flat Ge (444) mono-

^{a)}Electronic mail: spereira@fis.ua.pt

chromator and horizontal divergence slits with a width of 100 μm and a height of 2 mm select $\text{Cu K}\alpha_1$ radiation. The instrumental angular resolution is ~ 30 seconds of arc. RBS measurements were performed with a 1 mm collimated beam of 2.0 MeV $^4\text{He}^+$ ions. Samples were mounted on a computer-controlled two-axis goniometer with an accuracy of $\pm 0.01^\circ$. The backscattered particles were detected at 160° , with respect to the beam direction, using silicon surface barrier detectors located in the standard Cornell geometry, with a resolution of 12 keV.

In thin epitaxial semiconductor alloy films, gradients of strain and chemical composition may both lead to a variation of interplanar separations. If such gradients occur within the scattering volume, they broaden the reciprocal lattice points (RLPs). For symmetric (h and $k=0$) Bragg reflections, only variations in lattice constant perpendicular to the sample surface can be detected. The direction of RLP broadening along the surface normal does not distinguish its physical origin in this case. Uncertainties on the In content, and possible false indications of partial phase decomposition may result when only symmetrical x-ray reflections are considered, as recently discussed.^{6–8}

However, in the asymmetric case, the directions of elongation of the RLP due to strain and composition gradients differ significantly.⁹ An opportunity to separate the two effects arises from the fact that an asymmetrical RSM contains information on the in-plane and out-of-plane lattice constants. When the measurements are on an absolute scale, any pair of coordinates (q_x, q_z) in the map corresponds to a pair of lattice constants (a, c) of the wurtzite structure given by $a = (8\pi/3) \cdot (h^2 + k^2) / q_x$ and $c = 2\pi \cdot l / q_z$. The RSMs used in this work are not referred to the GaN RLP position but placed on an absolute scale.¹⁰ Note that the strain in the GaN buffer grown on sapphire changes during the growth process due to its lattice mismatch and thermal incompatibility with the substrate. Therefore, the degree of relaxation should be defined independently from the strain status of the substrate: $R(x) = [a(L) - a_0(S)] / [(a_0(L) - a_0(S))]$, where $a(L)$ and $a_0(L)$ are the measured and relaxed in-plane lattice constants, respectively, of a layer of given composition, and $a_0(S)$ is the relaxed lattice constant of the substrate.

The ability to separate the effects of strain and composition from the distribution of the RLPs (its extent and orientation) can be best illustrated by considering hypothetical cases in which only one of the parameters changes. Let a film of constant composition x progressively relax as it grows. The induced lengthening of the RLPs should be along the direction on the RSM that preserves the relation between a and c for a particular value of x . Two such isocomposition lines along which relaxation varies from $R=0$ to $R=1$ are shown in Fig. 1, at the angles α_1 and α_2 with respect to the Q_z axis (surface normal).

The angle $\alpha_i(x)$ can be calculated analytically. In an InGa N layer the strain components ε_{zz} and ε_{xx} are defined as $\varepsilon_{zz} = [c - c_0(x)] / c_0(x)$ and $\varepsilon_{xx} = [a - a_0(x)] / a_0(x)$, where c and a are the measured lattice parameters, while c_0 and a_0 are the relaxed parameters given by Vegard's law. The lattice constants of relaxed InGa N are larger than those of the underlying Ga N buffer. Therefore, in the basal plane of the heterostructure, a biaxial strain is built which causes a dis-

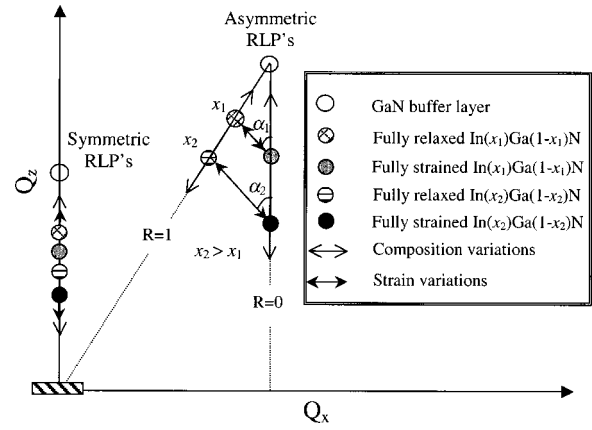


FIG. 1. Schematic diagram illustrating the effect of strain and composition gradients in the symmetric and asymmetric RLPs of $\text{In}_x\text{Ga}_{1-x}\text{N}$.

tortion of the hexagonal unit cell. In the epitaxial system under consideration, the c axis of the unit cell is normal to the substrate surface allowing a simplification of the tensor of the elastic moduli. The stress normal to the film vanishes and the following ratio between strains in the growth direction and basal plane is obtained:

$$\varepsilon_{zz} = -D(x)\varepsilon_{xx}, \quad (1)$$

with $D(x) = 2 \frac{c_{13}(x)}{c_{33}(x)}$, where $c_{i,j}(x)$ are the elastic constants linearly interpolated from the binary values. From the geometry in Fig. 1, $\tan \alpha(x) = (qx - q_0x) / (q_0z - qz)$. Substituting in Eq. (1) and using the expression for the angle φ between surface normal and the (hkl) planes,

$$\tan \varphi = \frac{c}{a} \sqrt{\frac{4(h^2 + hk + l^2)}{l^2}}.$$

$\alpha(x)$ can be expressed as a function of the elastic parameters, the reflection used, and the angle φ as

$$\alpha(x) = \arctan \left(\frac{1}{D(x)} \cdot \tan \varphi \cdot \frac{4(h^2 + k^2)}{l\sqrt{4/3(h^2 + hk + l^2)}} \right).$$

The input parameters necessary to perform the calculations are the Ga N ($c_{\text{GaN}} = 5.1850, a_{\text{GaN}} = 3.1892 \text{ \AA}$) and In N ($c_{\text{InN}} = 5.7033, a_{\text{InN}} = 3.5378 \text{ \AA}$) relaxed lattice parameters,^{11,12} and the elastic constants¹³ ($c_{13} = 103$ and $c_{33} = 405 \text{ GPa}$) for Ga N and ($c_{13} = 92$ and $c_{33} = 224 \text{ GPa}$) In N .

Now consider the hypothetical case, in which the alloy has a gradient of x and the relaxation is constant. The RLP will elongate along the line characteristic of this relaxation state, also illustrated in Fig. 1. In practice, a combination of both situations described will result in an extension of the RLP along some intermediate direction.

We use the concepts outlined above to examine the strain-composition features of a set of InGa N /Ga N films. It is important to note that symmetrical RSM (not shown) revealed no macroscopic tilts between the layers, as commonly verified in wurtzite nitride heterostructures.^{3–5} The asymmetrical RSMs measured around the (105) reflection, are shown in Fig. 2. Calculated isocomposition, full and zero relaxation lines are also shown. Diffraction corresponding to

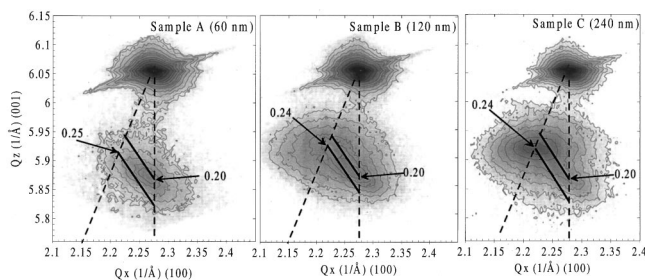


FIG. 2. Reciprocal space maps for the (105) reflections of the three InGaN/GaN layers with increasing thickness. The lines connecting the fully strained to the fully relaxed dashed lines indicate the calculated relaxation directions in the reciprocal space for various InN mole fractions.

the InGaN layer can be observed below the stronger GaN peak. Due to its great intensity, the GaN peak is followed by a detector streak.

With increasing layer thickness, the maximum of the InGaN RLPs progressively shifts from a fully strained to a fully relaxed position. In all the samples it is observed that the layers start growing pseudomorphic to GaN. However, not even the thinnest (60 nm) is fully coherent to GaN. Relaxation is progressive and the layers do not relax uniformly over depth. Even in sample C, which is mostly fully relaxed, it is observed that the first few monolayers remained coherent the GaN buffer. In fact, from samples B to C further growth leads to an increasing thickness of the relaxed part. This relaxation process is accompanied by an increase of mosaicity. The dislocations induced during relaxation will induce tilts in the mosaic blocks, the maximum of which is verified for the fully relaxed part of the layer. In fact, a slight tilt of main axis of the ellipse towards q_z in the relaxed part of sample C indicates that the mosaic structure in InGaN has a larger microscopic tilt contribution.^{10,14}

Careful comparison between the lengthening of the InGaN RLPs with the calculated pure relaxation directions, for specific values of composition, reveals an interesting feature of InGaN growth. As the films relax (grow) the indium content increases towards the surface. Note that in all samples the position of the RLPs in the coherent region, close to the GaN interface, indicates an In mole fraction of ~ 0.2 . Thereafter, a progressive shift of the RLP maximum towards isocomposition lines for larger x follows the layer relaxation. In fact, for all the samples the fully relaxed regions intercept the isocomposition lines calculated for $x \sim 0.24$ – 0.25 . This was the target composition in our films.

In order to ascertain that the In content increases along the growth direction, a detailed RBS study was performed. RBS allows an accurate determination of x free from the effects of strain, with depth resolution.¹⁵ A random RBS spectrum from sample B is shown in Fig. 3. Simulations of the RBS spectra were performed with RUMP.¹⁶ The simulation line obtained using a layer model with $x = 0.24$ provides a good fit only in the near surface region. For deeper InGaN regions the fit line is clearly overestimating the In and underestimating the Ga related signals. Nevertheless, letting the composition vary from 0.20 near the GaN interface to 0.24 close to the surface provides a good fit to the experiment as shown in Fig. 3. This is in excellent agreement with the results of RSM analysis.

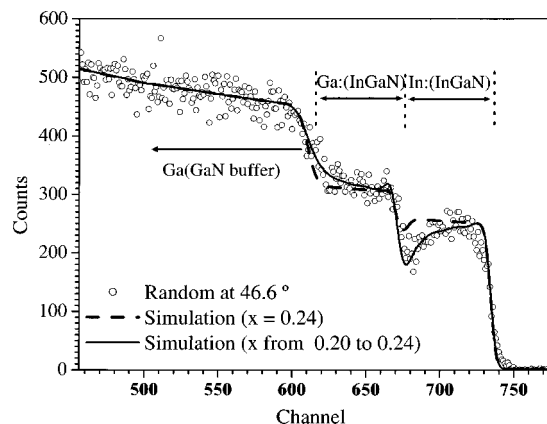


FIG. 3. Random RBS spectra for sample B. The dashed and solid lines represent the simulations obtained considering a uniform composition ($x = 0.24$) over depth and a varying composition (x from 0.20 to 0.24), respectively.

In conclusion, we have demonstrated the great potential of asymmetrical RSM to provide rich structural information on InGaN/GaN heterostructures. It is found that in InGaN epilayers grown on GaN strain may vary strongly with depth. The degree of relaxation can also influence the amount of In that is incorporated, particularly when trying to obtain films with large In mole fractions. Therefore, calibration procedures based on growth of thick (relaxed layers) can fail to provide a reasonable estimate of the In content in ultrathin layers such as those used in quantum wells, even when these are grown under the same nominal conditions.

¹S. Nakamura, J. Cryst. Growth **202**, 290 (1999).

²*Properties, Processing and Applications of Gallium Nitride and Related Semiconductors*, edited by J. H. Edgar, S. Strite, and I. Akasaki, INSPEC, 1999, A 7.11, p. 264.

³Z. Liliental-Weber, M. Benamara, J. Washburn, J. Z. Domagala, J. Bak-Misiuk, E. L. Piner, J. C. Roberts, and S. M. Bedair, J. Electron. Mater. **30**, 439 (2001).

⁴E. Zielinska-Rohozinska, J. Gronkowski, M. Regulska, M. Majer, and K. Pakula, Cryst. Res. Technol. **36**, 903 (2001).

⁵S. Pereira, M. R. Correia, E. Pereira, K. P. O'Donnell, C. Trager-Cowan, F. Sweeney, E. Alves, A. D. Sequeira, and I. M. Watson, Phys. Status Solidi B **228**, 59 (2001).

⁶S. Pereira, M. R. Correia, T. Monteiro, E. Pereira, E. Alves, A. D. Sequeira, and N. Franco, Appl. Phys. Lett. **78**, 2137 (2001).

⁷S. Pereira, M. R. Correia, E. Pereira, K. P. O'Donnell, E. Alves, A. D. Sequeira, and N. Franco, Appl. Phys. Lett. **79**, 1432 (2001); *ibid.* **80**, 337 (2002).

⁸M. Schuster, P. O. Gervais, B. Jobst, W. Hösler, R. Averbeck, H. Riechert, A. Iberl, and R. Stömmer, J. Phys. D **32**, A56 (1999).

⁹H. Heinke, S. Einfeldt, B. Kuhn-Heinrich, G. Plahl, M. O. Möller, and G. Landwehr, J. Phys. D **28**, A104 (1995).

¹⁰P. F. Fewster, ISBN 1-86094-159-1 (Imperial College Press, London, U.K., 2001).

¹¹T. Detchprohm, K. Hiramatsu, K. Itoh, and I. Akasaki, Jpn. J. Appl. Phys. **31**, L1454 (1992).

¹²W. Paszkowicz, Powder Diffr. **14**, 258 (1999).

¹³A. F. Wright, J. Appl. Phys. **82**, 2833 (1997).

¹⁴R. Chierchia, T. Bottcher, S. Figge, M. Diesselberg, H. Heinke, and D. Hommel, Phys. Status Solidi B **228**, 403 (2001).

¹⁵S. Pereira, M. R. Correia, E. Pereira, K. P. O'Donnell, C. Trager-Cowan, F. Sweeney, and E. Alves, Phys. Rev. B **64**, 205311 (2001).

¹⁶L. R. Doolittle, Nucl. Instrum. Methods Phys. Res. B **9**, 344 (1985).